

## ***Designing of Battery System and Study of Anode Alloy Materials for Improved Lithium Battery Performance***

---

*Final Report (05/25/11) — Dr. Paul Kohl, Hyea Kim, Johanna Stark*

*The views, opinions, and/or findings contained in this report are those of the author(s) and should not be construed as an official Department of the Army position, policy, or decision, unless so designated by other documentation.*

The Statement of Work for this program is divided into Task A and B.

Objectives:

- Task A: Johanna Stark
  - Identify appropriate lithium alloy anode (with sodium and/or Potassium) to prevent dendrite formation.
- Task B: Hyea Kim
  - Study new battery design incorporating ceramic membrane with improved safety and performance.

## Task A: Ionic Liquid Electrolyte and Lithium Alloy Anode

The deposition and re-oxidation of lithium metal is of interest for its potential use in lithium metal-anode batteries. The lithium-metal battery has the highest possible theoretical capacity. The use of the lithium redox process would eliminate the need for an anode structure, such as carbon or silicon, thus lowering cost and reducing assembly complexity. However, dendritic growth during repeated cycling is an efficiency and safety concern because dendrites can short circuit the anode and cathode (safety concern) and can become isolated from the cathode (efficiency concern). Anode-cathode short circuits are especially dangerous with a flammable organic electrolyte. In addition, lithium's instability within the electrolyte limits cycle life. The formation of a stable, solid electrolyte interface (SEI) is necessary to lower the degree of self-discharge. However, an SEI is not a realistic option on a high surface-area, dendritic surface. Thus, the goal of this effort is to deposit lithium in a non-dendritic form with a stable SEI layer.

Previous work has shown that cycle life can be extended by assembling and pressurizing a coin cell, but this does not address the fundamentals of dendrite formation(1). Restricting the dendrite volume and applying pressure forces denser dendrite growth, but the underlying driving force to grow dendrites is not eliminated. In this task, we studied the effect of alloying the lithium metal with a small amount of sodium in order to suppress dendritic growth. It is thought that the alloying of lithium through co-deposition would alter the rate or mechanism of dendrite growth and thus eliminate the problem. We hope to learn information about the mechanism of dendrite growth so as to better evaluate options for controlling the deposit. Further, we propose to study the use of ionic liquids as the electrolyte for deposition to mitigate the flammability issue.

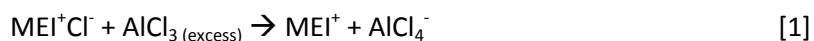
Although the non-dendritic growth of lithium addresses some of the safety issues, the instability of lithium in contact with the electrolyte causes capacity loss through self-discharge. In order to form a stable SEI layer between the metal deposit and the electrolyte, we investigated vinylene carbonate as an SEI forming agent. A 5wt% addition of vinylene carbonate to the electrolyte increased the cycling efficiency under voltage and current control to 90% (100 cycles).

In this task, we have shown demonstrated that (i) a dendrite-free lithium metal anode is feasible, and (ii) an ionic liquid with and SEI forming agent is an effective electrolyte for depositing lithium metal. The dendritic growth of lithium was eliminated by the addition of a small amount of sodium to the electrolyte. The addition of vinylene carbonate as an SEI forming agent improved the coulombic efficiency by forming a protective layer on the metal deposit and lower the reaction between the metal

and electrolyte. The coulombic efficiency for lithium metal deposition/oxidation was improved to 90% as measured for over 100 cycles without dendrites.

#### *Methyl-ethyl-imidazolium chloroaluminate (MEIC)*

The MEIC was formed by buffering an acidic melt of  $\text{MEI}^+ \text{Cl}^-$  and  $\text{AlCl}_3$  with either lithium chloride or sodium chloride depending on the desired electrolyte.



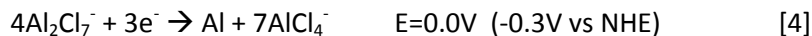
The  $\text{AlCl}_3$ :MEIC ionic liquid was made by slowly mixing the two components in a 55:45 molar ratio until only a clear liquid remained (Equation 1 and 2). This liquid was dried under vacuum for 8 h followed by the addition of 100% excess metal chloride to ensure a completely buffered melt (Equation 3). In order for this melt to give reversible plating/dissolution, ~0.005 wt% of  $\text{SOCl}_2$  was added to each electrolyte. Ionic liquids containing both sodium and lithium salts were mixed by volume from separate single salt mixtures.

For electrochemical testing, the working electrode was a 0.5 mm tungsten wire and the counter electrode was a 1 mm tungsten wire. Both were encased in borosilicate glass and polished before each use.

#### *Tri-methyl butyl ammonium bis(trifluoromethanesulfonyl)imide (QATFSI)*

Tri-methyl-butyl-ammonium bis(trifluoromethanesulfonyl)imide (QATFSI) electrolytes were made by adding the metal TFSI salt to the ionic liquid. LiTFSI was commercially available. Sodium bis(trifluoromethanesulfonyl)imide (NaTFSI) was synthesized by the reaction of bis(trifluoromethanesulfonyl)imide (HTFSI) with a 1M NaOH solution until the pH was neutral. The solution was heated to 60°C and dried under vacuum for 8h to remove all water. The resulting NaTFSI powder was transferred to the glovebox. After the appropriate metal TFSI salt was dissolved in QATFSI, the ionic liquid was dried under vacuum for several hours before use.

The reference electrode for all experiments was an aluminum wire immersed in a 60:40 mol ratio  $\text{AlCl}_3$ :MEICl melt in a fritted glass tube. The electrochemical couple is between the acidic chloroaluminate species and the metallic Aluminum, as described in Equation 4.



Electrochemical measurements were carried out in a glass cell with electrodes spaced less than 1 cm apart. Scanning electron microscopy was used to study the morphology of different deposits. Metal was deposited on the appropriate foil attached to a wire. Images were taken with a Zeiss Ultra 60 SEM.

*Characterization of MEIC melts*—sodium and lithium buffered MEIC melts were prepared to study their deposition/dissolution properties and deposit morphology. The cyclic voltammograms shown in Figure 1 demonstrate metal reduction on the negative going scan and oxidation on the positive going scan.

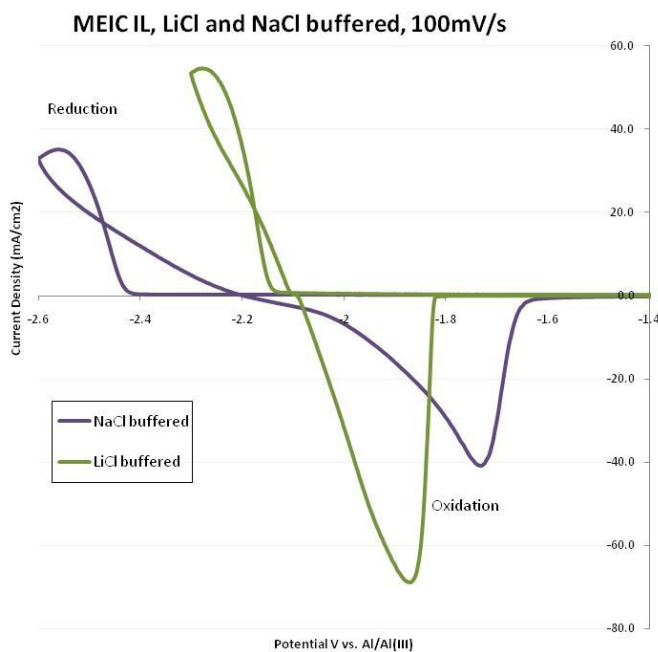


**Figure 1: CV of lithium and sodium buffered MEIC melts. A coulombic efficiency was calculated based on the area of the reduction and oxidation peaks. lithium showed an efficiency of 90% and sodium showed an efficiency of 82%. The Scan rate was 100mV/s.**

An interesting feature of this particular ionic liquid is that the reduction potentials are shifted positive from their standard potentials. lithium is reduced at -2.15 V and sodium at -2.4 V vs. Al/Al(III). This shift is due to an interaction with the chloroaluminate anion. In this particular ionic liquid, lithium

reduces at a more positive potential than sodium. A coulombic efficiency can be calculated from the area of the reduction and oxidation peaks. This coulombic efficiency was 90% for lithium and 82% for sodium. For lithium, the loss of efficiency can be attributed to reaction with the electrolyte as well as lithium's dendritic behavior. Sodium also reacts with the electrolyte, but the loss of efficiency here is primarily due reduction of the electrolyte. An unbuffered acidic MEIC melt is reduced at -2.2 V on a tungsten electrode. The addition of  $\text{SOCl}_2$  to the melt increases this window to -2.4 V, which coincides with the sodium reduction potential. The 200 mV overpotential is attributed to the nucleation of Na on Tungsten. sodium also shows a slow onset for the oxidation peak compared with lithium. This could be because of an unfavorable exchange current.

The goal of this work was to study ionic liquids containing both sodium and lithium salts to see whether such a combination could help suppress the dendritic growth of lithium. A 1:1 volume mixture of lithium buffered MEIC and sodium buffered MEIC was mixed and its behavior studied using cyclic voltammetry. By varying the switching potential, the behavior shown in Figure 2 is observed.

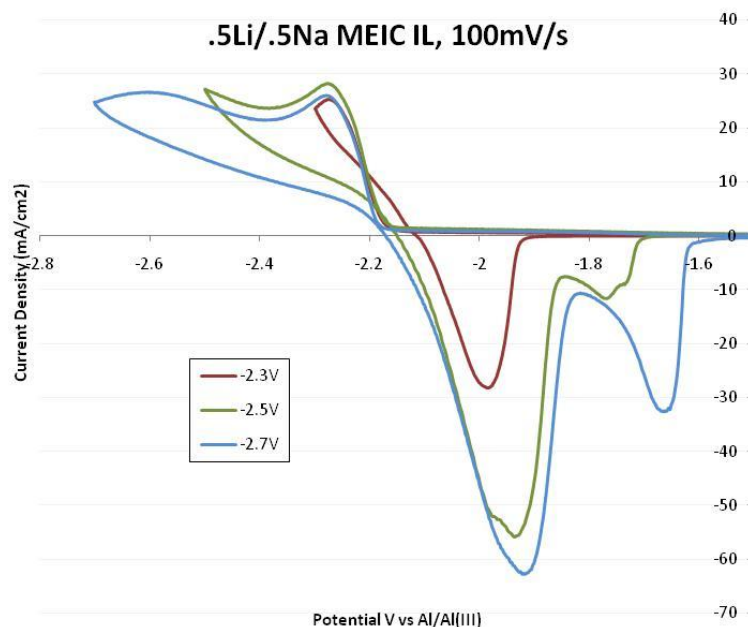


**Figure 2: Cyclic voltammetry study of a 1:1 mixture of sodium and lithium buffered MEIC melts. The scan rate was 100mV/s.**

When the switching potential is positive of -2.3 V, only a single peak is visible. The CV has many features in common with the CV of a lithium buffered melt such as the reduction potential of -2.15 V and a sharply defines oxidation peak. As the switching potential goes to a more negative value, a second oxidation peak appears at -1.7 V. This peak matches closely with the behavior of a sodium buffered melt in potential and has a similar shallow-sloped onset.

To identify the composition of these peaks, inductively coupled plasma emission spectroscopy (ICP-ES) was carried out on several samples deposited from this ionic liquid. The error in these experiments came from incomplete removal of the electrolyte, which skewed the elemental analysis. In addition, the peaks cannot be separated due to the slow onsets of the more positive peak, also making an exact determination difficult. The results of the ICP analysis are shown in Table 1.

	Li (ppm)	Na (ppm)	Li (%)	Na (%)
1) 1M Li, contaminated	22.1	2.24	90.8	8.2
2) 50%Li/50%Na dep at -2.2V	13.9	1.67	89.3	10.7
3) 50%Li/50%Na dep at -2.6V	5.46	22	19.9	80.1

**Table 1: ICP-ES results showing elemental analysis of deposits from MEIC ionic liquid.**

In order to establish a baseline, lithium was deposited from a 1M Li MEIC ionic liquid. The sample was then dipped in a sodium ionic liquid to simulate contact with the electrolyte. This introduced a 10% error in the elemental analysis. The second and third samples were taken from a 0.5Li/0.5Na MEIC ionic liquid at different potentials. At -2.2 V, only the more positive peak appears and we see that the deposit is mostly lithium. At -2.6 V, a CV clearly shows two peaks and the elemental analysis shows that at this potential, the deposit is 80% sodium. We can thus conclude the more positive peak seen in CV is sodium, or a sodium rich alloy.

To further understand this double peak, deposit morphology was analyzed by examining metal deposited at several different current densities. SEM images of these deposits are shown in Figure 3.

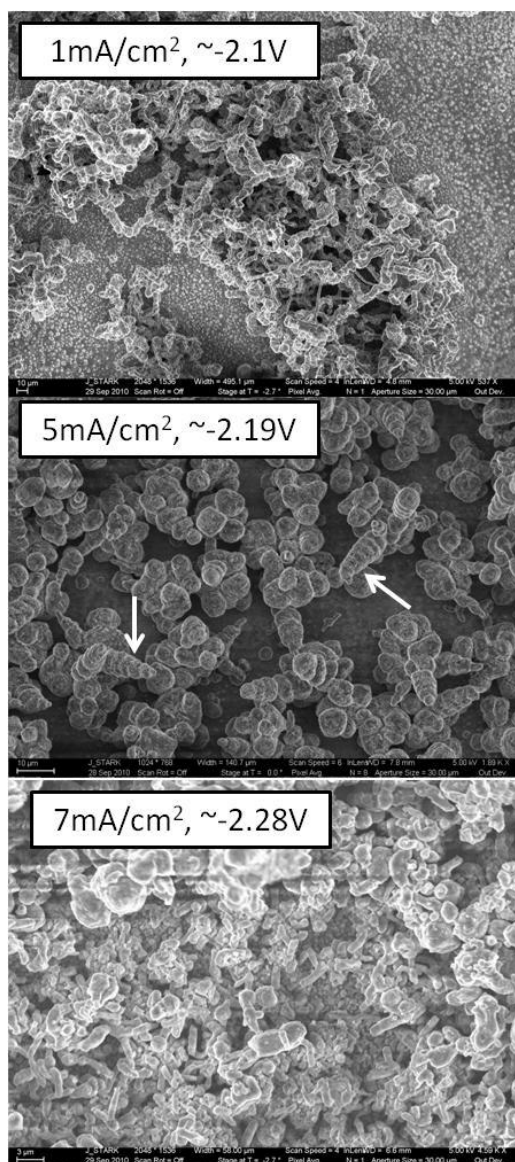


**Figure 3: SEM images of deposits from a 90%Li/10%Na buffered MEIC melt. Metal was deposited at the current shown until a charge of 5C/cm<sup>2</sup> was reached.**

The low current deposit at 1 mA/cm<sup>2</sup> looks identical to the deposit from a lithium buffered melt. Curling dendrites form moss-like structures on the substrate surface. At 5 mA/cm<sup>2</sup> and 7 mA/cm<sup>2</sup>, a lithium deposit from MEIC would show straight, sharp needles but the melt containing 10% sodium showed only small, stunted needles at 5 mA/cm<sup>2</sup>. At an even higher current of 7 mA/cm<sup>2</sup>, only elongated structures were visible, and no sharp, pointed dendrites could be found.

Based on the potentials recorded during the steady state deposition of these structures, the disappearance of dendrites coincides with the appearance of the second oxidation peak on the CV scans. ICP results indicate that the appearance of the second peak coincides with an increase in sodium in the deposit. Thus it is likely that we are observing a co-deposition of sodium and lithium rather than

an alloying process. sodium can co-deposit with lithium, thus hindering the dendritic growth that would be detrimental for a battery application.

The purpose of suppressing dendritic growth was to increase the efficiency and cyclability from MEIC melts. Coulombic efficiencies were calculated from CV with various switching potentials. The results are presented in Figure 4.

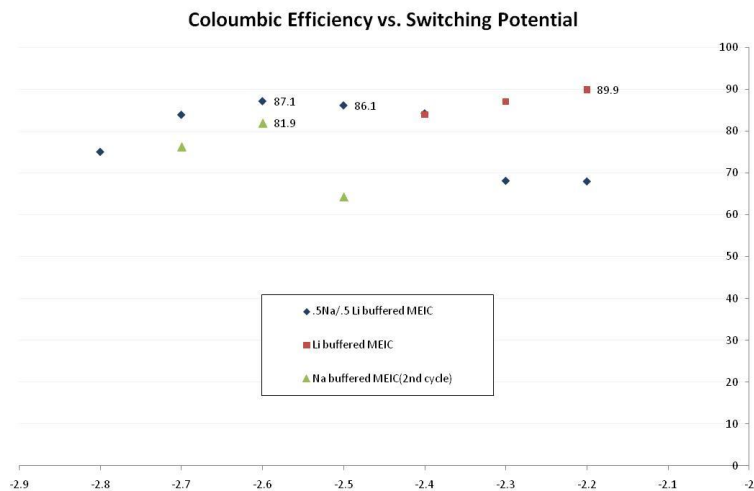
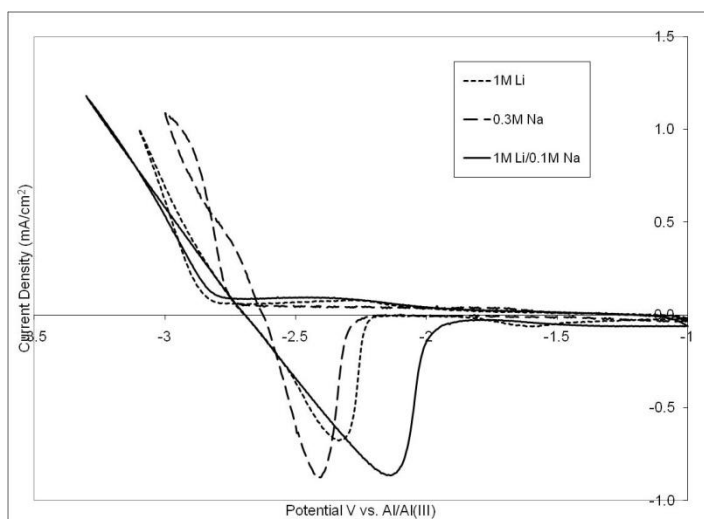


Figure 4: Coulombic efficiencies calculated from CV at different switching potentials.

The maximum coulombic efficiency for lithium is 90% and can be seen with a switching potential of -2.2V. Scanning to more negative potentials lowers the efficiency because of the onset of MEI<sup>+</sup> reduction. For sodium, the highest efficiency was 82% with a switching potential of -2.6 V. At -2.5 V very small peaks were recorded but background current was not negligible so the efficiency was lower. Again, going to more negative potentials lowered the efficiency because of reduction of the electrolyte. Shown along with the efficiencies for the single metal melts in Figure 4 are those of a 50%Li/50%Na melt. The maximum efficiency for this melt was 87% achieved at -2.6 V. This efficiency is, unfortunately, no higher than that of the lithium only melt. At the more positive potentials of lithium, the efficiencies could have been low because of the smaller concentration of lithium ions in the melt. There could be some suppressing effect caused by the sodium ions. The drop-off in efficiency at more negative potentials is again attributed to MEI<sup>+</sup> reduction.

Though dendrites were successfully suppressed in the MEIC system, the change in morphology did not lead to an increase in efficiency or cycle life. This makes the MEIC ionic liquid unsuitable for battery applications.

*Characterization of QATFSI Ionic Liquid*—TFSI based ionic liquids have better tolerance for water and oxygen contamination than their chloroaluminate counterparts. The stability window for trimethyl-ethyl-ammonium TFSI extends to -3.4 V, and has been previously shown to support reversible lithium and sodium couples. Electrochemical experiments were performed at a 305 stainless steel working electrode. Figure 4 shows the CV behavior of 1M Li<sup>+</sup> and 0.3M Na<sup>+</sup> in QATFSI. The low solubility of NaTFSI in QATFSI did not allow for testing at higher Na<sup>+</sup> concentrations.



**Figure 5: CV of 1M Li<sup>+</sup>, 0.3M Na<sup>+</sup>, and 1M Li<sup>+</sup>/0.1M Na<sup>+</sup> in QATFSI. Coulombic efficiencies were 55% for lithium, 50% for sodium, and 57% for the mixture. The scan rate was 10mV/s.**

Initial Cyclic Voltammetry and Chronopotentiometry of 1M Li<sup>+</sup> QATFSI ionic liquid did not look as promising as MEIC. The coulombic efficiency calculated from the CV cycle was 55% for lithium and 54% for sodium. Notable are the reduction potential of the two metals. Unlike in the chloroaluminate ionic liquid, lithium and sodium are -2.85 V and -2.75 V respectively; thus, using this ionic liquid would give a higher voltage final battery in comparison the chloroaluminate system.

In an attempt to alloy the two metals, a solution with 1M Li<sup>+</sup>/0.1M Na<sup>+</sup> QATFSI was mixed and dried under vacuum. The CV behavior of this ionic liquid, drawn in Figure 5, showed a coulombic efficiency of 57%. This efficiency is slightly higher than that of the 1M Li<sup>+</sup> electrolyte. Contrary to the chloroaluminate ionic liquid, this mixture only displayed a single peak, pointing towards an alloying process rather than a co-deposition of the two metals.

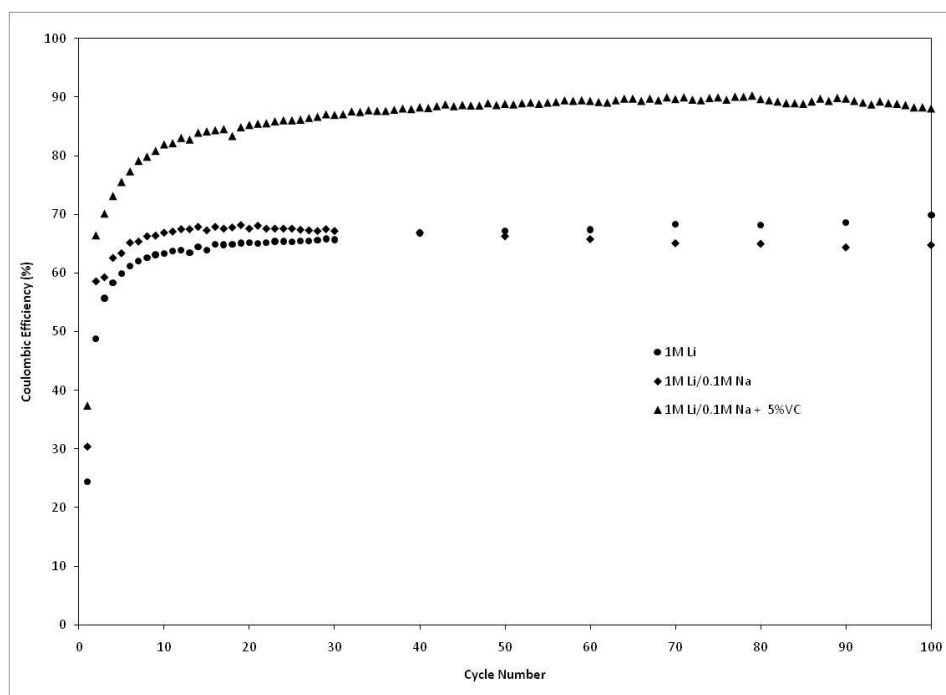
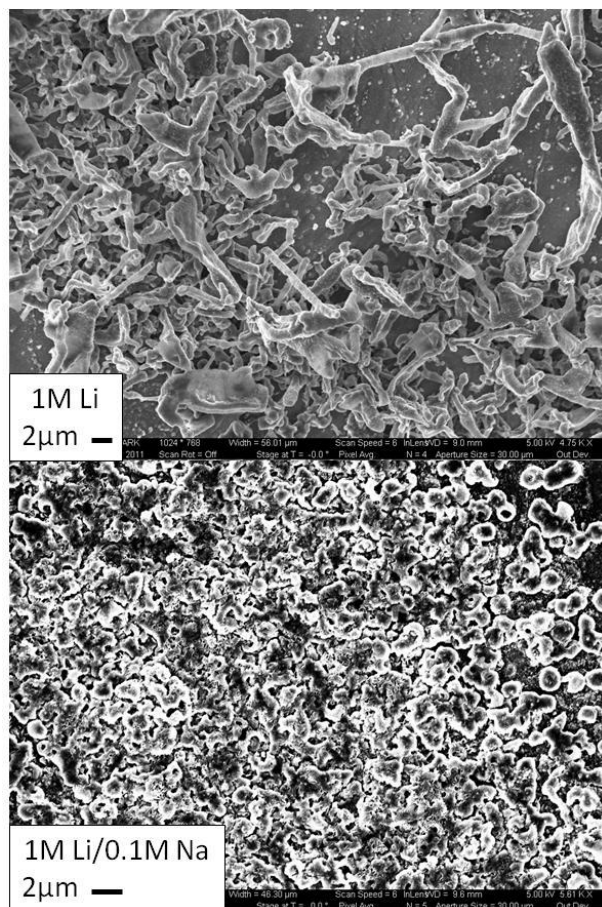


Figure 6: Cycling experiments at 0.1mA/cm<sup>2</sup> for 100s.

Chronopotentiometry experiments consisted of depositing for 100 s at 0.1 mA/cm<sup>2</sup> and then applying the same magnitude current of opposite polarity until the voltage reached -1.5 V. A 1M Li<sup>+</sup> QATFSI ionic liquid could maintain 70% efficiency for greater than 100 cycles. No significant performance improvement was seen using the ionic liquid mixture of 1M Li<sup>+</sup>/0.1M Na<sup>+</sup> in QATFSI compared to the 1M Li<sup>+</sup> ionic liquid. The coulombic efficiency reached 70% and dropped off very slowly.

While the cycling performance for the lithium and lithium/sodium ionic liquids was very similar, their deposit morphologies differ significantly. Figure 7 shows deposits from both ionic liquids. Lithium shows long dendrites 1-2 μm diameter. The 1M Li/0.1M Na ionic liquid however deposited as a porous, even film with no dendrites present. This is most likely an alloy deposit that contains both lithium and sodium. If lithium's dendritic growth is due to preferred deposition on a certain crystal face, the larger sodium atom would break up such growth, leaving a dendrite free deposit. This would normally lead to a better cycling performance, however, the sodium couple is not very efficient in QATFSI.

Chronopotentiometry experiments like those shown in Figure 6 gave only 50% for sodium. It is likely that the poor cycling efficiency of sodium negates the positive effect sodium has on the morphology.



**Figure 7: SEM images of deposit from a 1M Li electrolyte and a 1M Li/0.1M Na electrolyte. A constant current of  $0.5\text{mA}/\text{cm}^2$  was applied for 1000s for  $0.5\text{C}/\text{cm}^2$ .**

The poor cycling performance of Li-metal anodes can be attributed to poor SEI formation. While the large surface area, dendritic growth can be one barrier, lithium's reactivity with the electrolyte is another. In order to form this stable film, vinylene carbonate was evaluated for their effect on cycling efficiency. 5wt% VC was added to a 1M Li/0.1M Na QATFSI electrolyte. CV and chronopotentiometry tests were then carried out as described before. The coulombic efficiency recorded from CV was 90%, significantly higher than the lithium or lithium/sodium ionic liquids. Cycling performance also greatly improved. The coulombic efficiency reached 85% within 30 cycles and was steady at 90% through 100 cycles (Figure 6). This improvement is credited to less detrimental reaction between the deposit and the electrolyte. Vinylene carbonate can react with the deposit to form a stable film that prevents further reaction.

*Conclusion*—Two ionic liquids, MEIC and QATFSI, have been studied as battery electrolytes. Both have a large enough stability window to support lithium deposition and dissolution, making them candidates for lithium battery applications.

The approach to mitigating dendrite growth that currently prevents lithium metal anodes from being commercially viable, was to add a small amount of sodium to the ionic liquid. There are two possible mechanisms for that would prevent dendrite growth in such a mixture. First, it is possible to co-deposit the two metals. Because the sodium atom is larger than the lithium atom, a small amount of sodium can disrupt lithium's dendritic growth. A second possibility is to form an alloy of the two metals. This alloy can be potentially non-dendritic, even with a small amount of sodium, resulting in a smooth deposit.

A second problem is that lithium reacts with the electrolyte, causing capacity loss and blocking the substrate. This problem was approached with SEI forming additives. These additives can react with the deposited metal to form a stable, protective film that prevents further reaction.

In this work, we have shown that both MEIC and QATFSI support non-dendritic deposits by the addition of a small amount of sodium to a lithium-based ionic liquid. Additives were studied with QATFSI and it was shown that 5% vinylene carbonate added to a 1M Li/0.1M Na ionic liquid could help build a stable SEI, resulting in a cycling efficiency of 90% over 100 cycles.

## TASK B: New Battery Design with Ceramic Membranes

The goal of Task B is to create a new battery design incorporating ceramic membranes (LiSICONs). Ceramic membranes attract much attention toward solving the safety problem in commercialized lithium-ion batteries (LiBs). In order for the LiSICONs to perform lithiation/delithiation, it was required to use a wetting agent to reduce the interfacial resistance between LiSICONs and electrodes. Ionic liquids have been studied as a wetting agent so that the lithium ion-batteries can be utilized at high temperature as well. The charge /discharge capacity and efficiency of the LiBs have been investigated at 25C, 50C and 80C. AC impedance was used to understand the cell behavior.

Among various types of ionic liquids, N-methyl-N-propylpyrrolidinium bis(fluorosulfonyl)imide ( $\text{PYR}^+\text{FSI}^-$ ) was chosen as a wetting agent, because FSI based ionic liquids have been reported to show excellent reversible lithiation/delithiation without any usage of SEI former additive(2). 0.5M LiTFSI/PYRFSI was used and tested at 25C, 50C and 80C. Impedance study showed that the 0.5M LiTFSI/PYRFSI reduced the interfacial resistance significantly and graphite anode was largely responsible. The overall impedance was decreased with temperature as expected. At 25C and 50C, two semicircles were observed. The first semicircle at high frequency was for the grain boundary RC circuit and the second arc was for the combination of the both electrodes double layer capacity. At 80C, only one semicircle was observed indicating that the impedance of grain boundary is small at 80C. As increasing the temperature, the IR drop due to the LiSICON was reduced because the LiSICON conductivity improved with temperature so the capacity and efficiency increased.

Lithium salt concentration in ionic liquids has been known to change the conductivity/viscosity and the reduction potential of the mixture. The effect of salt concentration on cell performance was investigated using 0.50M, 0.75M and 1.00M. It was found out the reduction potential was shifted negatively with the concentration. 0.75M provided higher reversible capacity than 0.5M even with its lower conductivity because 0.5M reduced earlier consuming more graphite to react resulted in high irreversible capacity. 1.0M showed lower performance than 0.75M, since the conductivity of 1.0M was lower so it could not fully lithiate.

Finally, at 80C, the cell with LiSICON using 0.75M LiTFSI/PYRFSI as a wetting agent showed comparable capacity (310mAh/g) to organic solvent electrolyte. The capacity was stable over cycles and the efficiency was 99.7%. Further studies are being conducted to operate the cells at higher temperature of 120C. Li-metal is proposed as a second possible anode with LiSICON for future works.

## 1. Characterization of LiSICONs

Among the different types of ceramic membranes, LiSICON, which has been known to have fairly high conductivity, was received from CeramaTech. LiSICON is a NaSICON type lithium ion conducting ceramic membrane shown in Figure B1. The diameter is 2.6 cm and the thickness is 500  $\mu\text{m}$ .

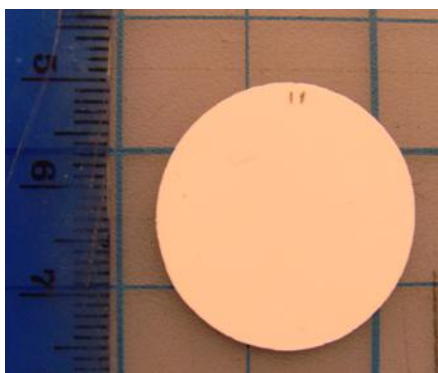


**Figure B1: LiSICON**

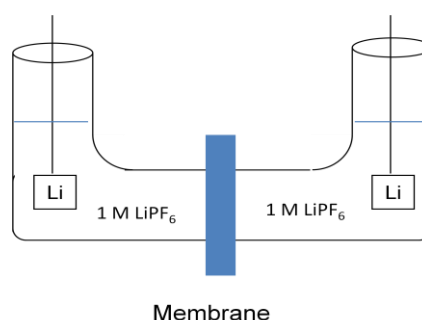


**Figure B2: Conductivity measurement**

The ionic conductivity of the membrane was measured by AC impedance performed with a Perkins Elmer PARSTAT 2263 potentiostat. The membrane was placed between the two glass cells shown in Figure B2 and a 1M  $\text{LiPF}_6$  /EC-DMC (vol. 1:1) electrolyte solution was added until the membrane was fully submerged. The two lithium electrodes were placed on either side of the membrane at a fixed distance from the face of the membrane and connected to a potentiostat. The ionic conductivity of LiSICON was  $2 \times 10^{-3}$  S/cm.

## 2. Organic solvent performance with commercial graphite electrodes

The charge and discharge capacity of the graphite electrodes (purchased from MIT Corporation) was measured at C/20 for reference as shown in Figure B3. As an electrolyte, 1M  $\text{LiPF}_6$  /EC-DMC (vol. 1:1) was used. The first charge capacity was 371.3mAh/g, which is very close to the theoretical value of 375mAh/g. The 1<sup>st</sup> discharge capacity was 324.8mAh/g, indicating that the irreversible capacity is 46.5mAh/g. The cycle was stable for 3 cycles with 97% of efficiency.

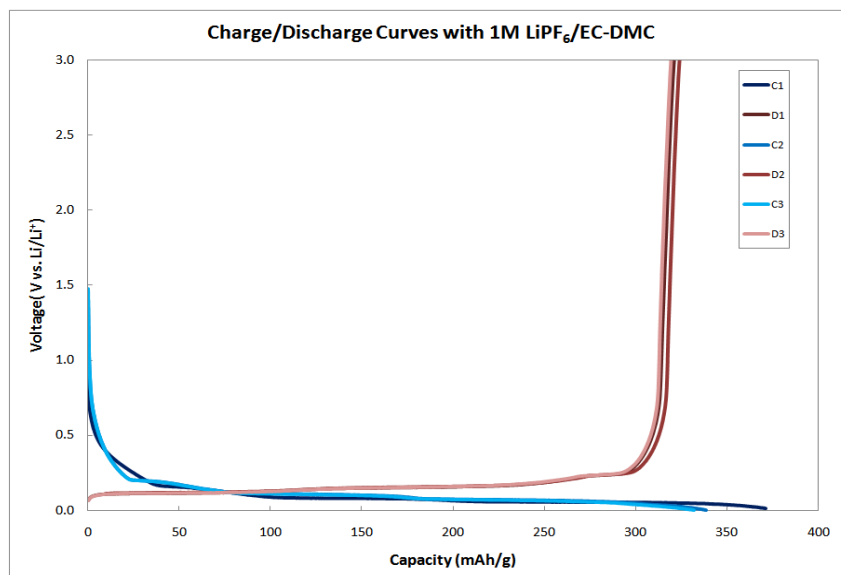


**Figure B3: Charge and discharge capacity for the graphite electrode**

### 3. LiSICON Insertion

Liquid electrolyte (1M LiPF<sub>6</sub> /EC-DMC (vol. 1:1)) was replaced with a LiSICON as shown in Figure B4 and tested as an electrolyte with the graphite anode.

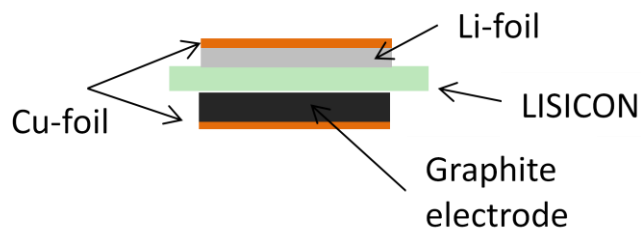


**Figure B4: Half-cell set up with LiSICON**

The CV result with the LiSICON is shown in Figure B5. The overall current with the LiSICON was lower compared to the current with a liquid electrolyte and no lithiation/delithiation peak was observed. It seemed that the large IR drop due to the LiSICON and poor contact between the electrodes and the LiSICON could be the reason for the low performance. Impedance analysis was conducted to understand the problems.

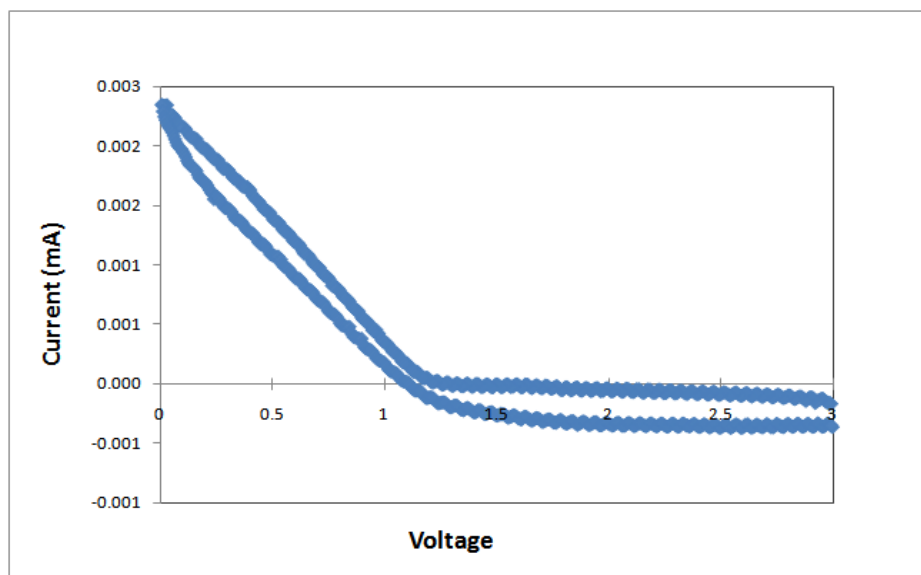


Figure B5: CV with LiSICON at 10mV/s

#### 4. Impedance analysis on interfacial resistance

##### 4-1. Impedance result with the organic solvent

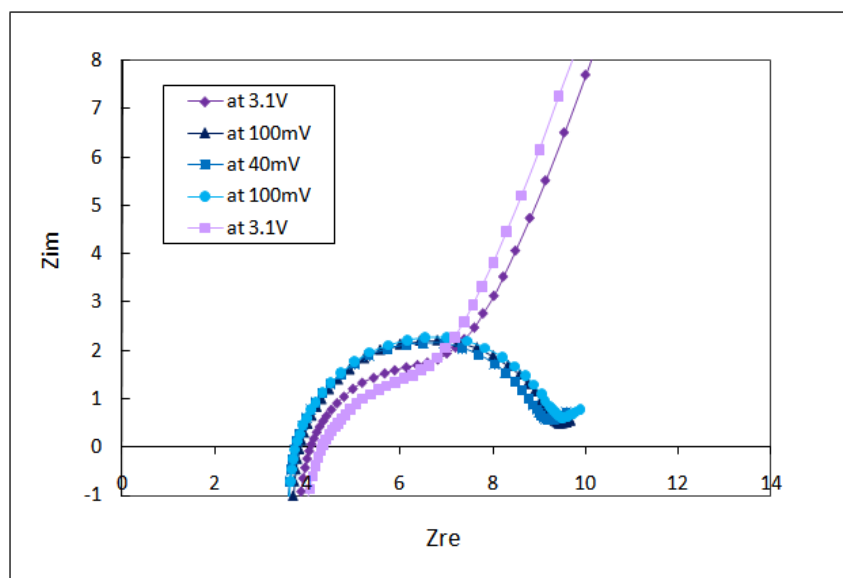
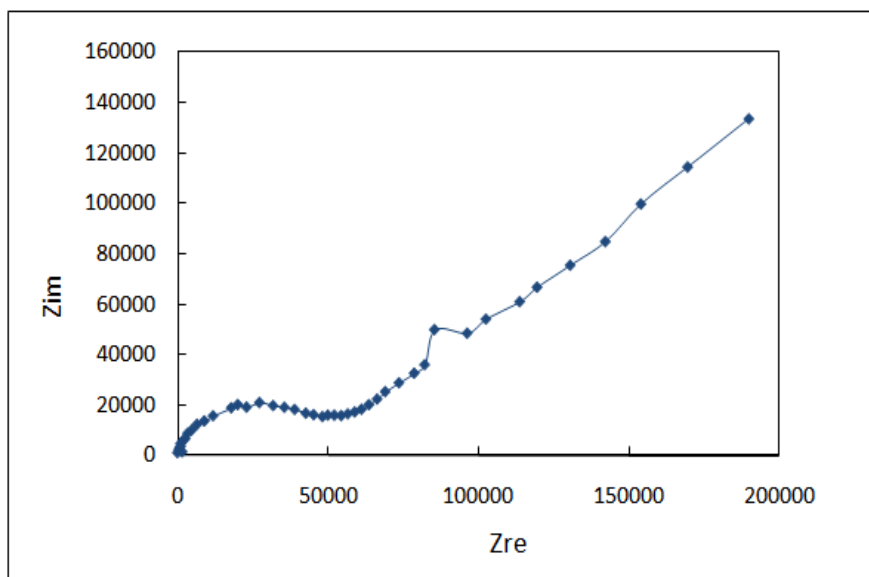


Figure B6: Impedance with the liquid electrolyte in a half-cell configuration

For reference, impedance test was performed for the half-cell with the organic solvent. Figure B6 showed the impedance at a charge state of 100mV and 40mV, and at a discharge state of 3.1V. A clear semicircle was observed. The resistance from the liquid electrolyte is around 4 ohms and the charge transfer resistance is around 6 ohms.

#### 4-2. Impedance result with the LiSICON



**Figure B7: Impedance with the LiSICON in a half-cell configuration**

Impedance test was performed in a same manner for the half-cell with the LiSICON. Figure B7 showed that the cell has an unacceptably high resistance compared to Figure B6. The impedance at a charge state was impossible to measure, because the lithiation did not occur.

#### 4-3. Three different half-cell configurations

The extremely high impedance observed in Figure B6 could be due to the poor contact of the LiSICON with either/both the counter electrode (lithium metal) or/and the contact with the working electrode (graphite anode). Three different half-cell configurations were designed, shown in Figure B8, to determine which interface is largely responsible for the high resistance. Liquid electrolyte (1M  $\text{LiPF}_6$  /EC-DMC (vol. 1:1)) was introduced to reduce the interfacial contact resistance between the electrode and LiSICON. Configuration 1(Con1) does not include any solvent, configuration 2(Con2) has liquid electrolyte at the lithium metal side, and configuration 3(Con3) has liquid electrolyte at the graphite anode side. When the electrode has the liquid electrolyte in the contact with the LiSICON, the interfacial resistance can be minimized.

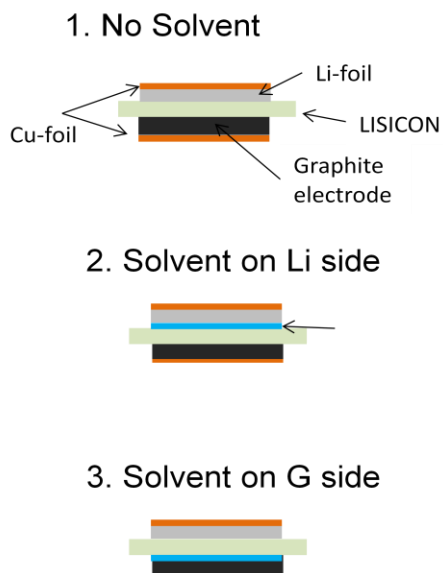


Figure B8: Three different half-cell configurations

#### 4-4. Impedance for the three half-cell configurations

Figure B9 showed the overall impedance of the Con 2 was lower than the Con 1. The Con 3 had the lowest impedance, indicating that the interfacial resistance with the LISICON can be reduced by the introduction of some contact agent and the resistance at the side of a graphite anode was largely responsible for the high resistance

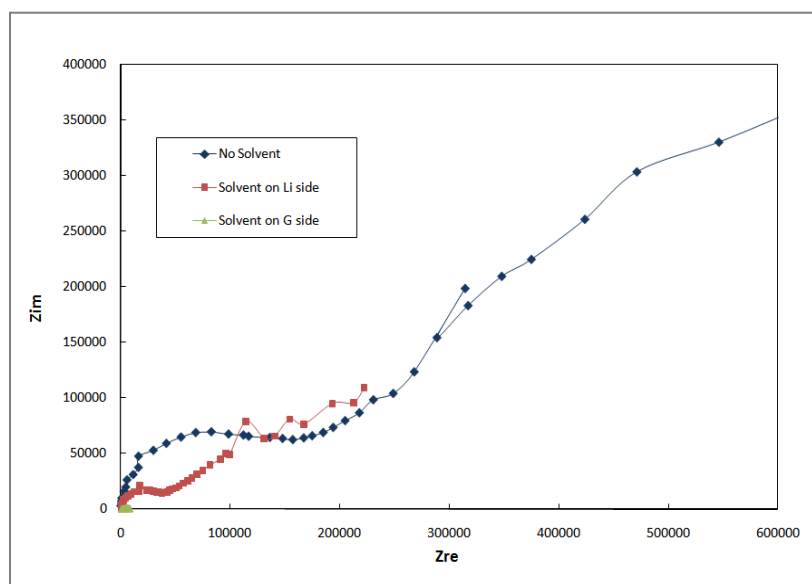


Figure B9: Impedance results for the three different half-cell configurations

### 5. Ionic liquid as a contact agent

Impedance results showed that the interfacial resistance between the electrodes (especially, graphite anode) and the LiSICON was too high to lithiate/delithiate. The contact resistance needs to be reduced. Liquid electrolyte such as 1M LiPF<sub>6</sub>/EC-DMC (vol. 1:1) can be used as a contact agent as shown in Figure B8, but the organic solvent is flammable and it does not match to the purpose of using a LiSICON. However, ionic liquid can be a possible contact agent, since it is already shown that some ionic liquids can be used as an electrolyte for lithium ion batteries and it is not flammable. Also, high temperature application can be utilized.

Literature search provided some information for choosing a right ionic liquid combination. Decomposition of the ionic liquids on the graphite anode has restricted their application in Li-ion batteries. When TFSI<sup>-</sup> is used as an anion, no lithiation occurs so an SEI layer forming agent such as VC is required. Ishikawa et al. (3) found that FSI<sup>-</sup> showed a reversible lithiation. While EMI<sup>+</sup>-FSI<sup>-</sup> has a higher reactivity toward LiCoO<sub>2</sub>, Pyr<sub>1R</sub><sup>+</sup>-FSI<sup>-</sup> seems to be the most possible candidate. Based on the information, two ionic liquids, EMI<sup>+</sup>-FSI<sup>-</sup> and Pyr<sub>1R</sub><sup>+</sup>-FSI<sup>-</sup> were chosen to be tested as a contact agent.

#### 5-1. Reactivity of the LiSICON with lithium metal

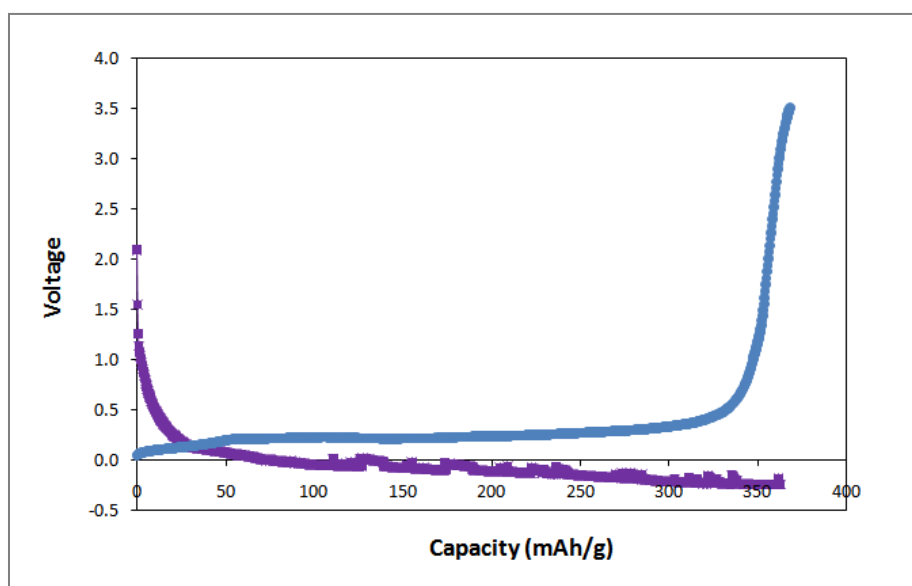


Figure B10: The 3<sup>rd</sup> charge/discharge curves of Con 3 at C/20

During the charge/discharge test with Con3, a black layer formed on the surface of the LiSICON on Li-metal side and a similar observation was reported by Kennedy and Zang(4). Also, Knauth et al.(5) reported that LiSICON is highly reactive with Li metal. Figure B10 showed an unstable charge curve for the 3<sup>rd</sup> charge/discharge test for Con3. However, the black layer was not observed during the test of

Con2, which has liquid electrolyte between the Li-metal and LiSICON. The direct contact of lithium metal to LiSICON might be unfavorable. Further tests to confirm the reactivity of the LiSICON with lithium metal will be conducted for this lithium battery study.

### 6. Reversibility and efficiency of $\text{Pyr}_{13}^+ \text{-FSI}^-$

Cyclic voltammetry was performed to check the reversibility of lithiation and delithiation using  $\text{Pyr}_{13}^+ \text{-FSI}^-$  as an electrolyte. Figure B11 shows the cyclic voltammetry of 0.5M LiTFSI/  $\text{Pyr}_{13}^+ \text{-FSI}^-$  and 1.0M LiPF<sub>6</sub>/EC-DMC on graphite electrodes. FSI- based ionic liquid showed clear reduction (lithiation) and oxidation (delithiation) peaks with 84% efficiency (compared to 97% efficiency with organic solvent).

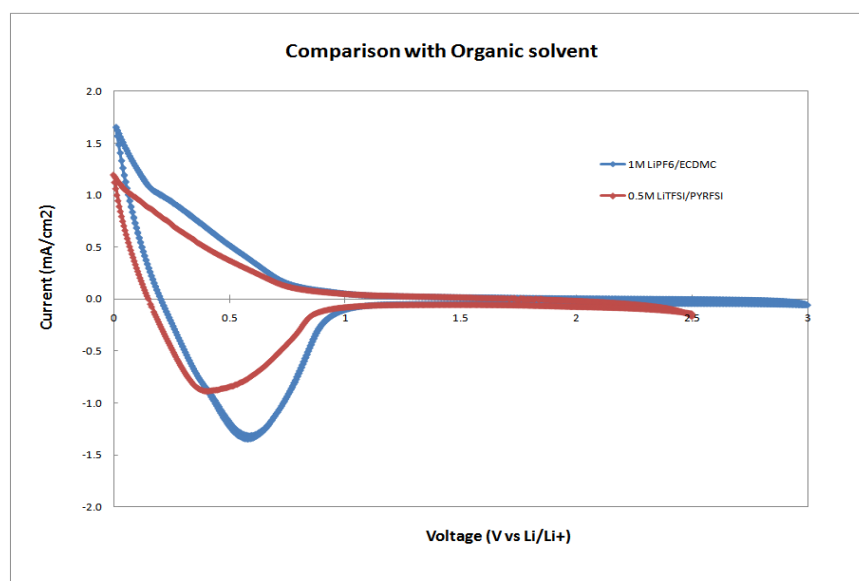


Figure B11: Cyclic voltammetry of  $\text{Pyr}_{13}^+ \text{-FSI}^-$

### 7. $\text{Pyr}_{13}^+ \text{-FSI}^-$ as a wetting agent with LiSICON

Previously, LiSICON was used as a solid electrolyte and it was impossible to lithiate and delithiate due to the high contact resistance. When 0.5M LiTFSI/  $\text{Pyr}_{13}^+ \text{-FSI}^-$  was used as a wetting agent, lithiation and delithiation were possible. Figure B12 shows four cycles with LiSICON using 0.5M LiTFSI/  $\text{Pyr}_{13}^+ \text{-FSI}^-$  as a contact agent at 25C. As expected, there was an high IR drop around 0.5V due to the high resistance of the LiSICON. The big reduction at 0.2V in the first charge curve (C1) is for the SEI formation (electrolyte reduction on graphite electrodes). The first discharge capacity (D1) was low (30mAh/g) due to the dominant SEI formation reaction versus lithiation during the first charge. From the second charge/discharge, the lithiation becomes dominant. The discharge capacity increased from

30 to 240mAh/g and remained same at 4<sup>th</sup> cycle. It should be noted that the potential window was not set for this experiments to know how much IR drop exist.

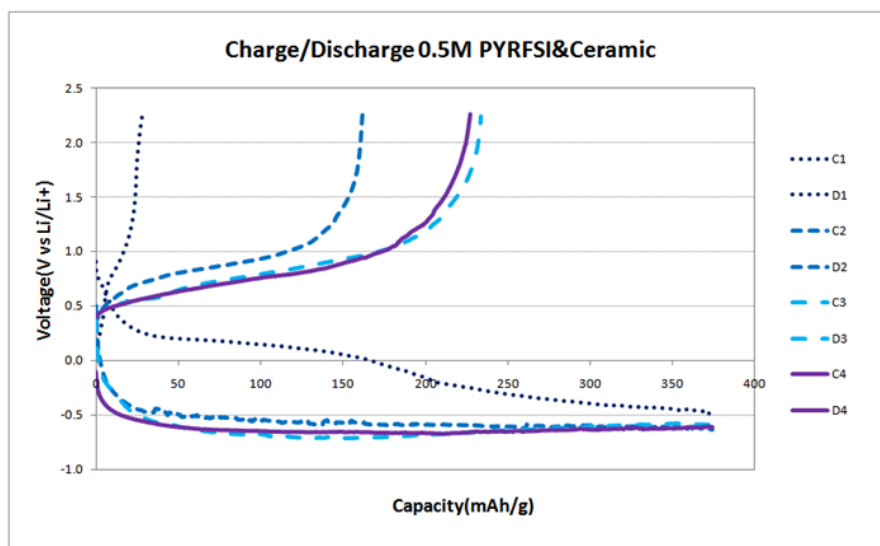


Figure B12: Charge/Discharge cycles of the cell with LiSICON using 0.5M LiTFSI/ Pyr<sub>13</sub><sup>+</sup>-FSI<sup>-</sup> as a contact agent (25C)

### 8. Higher temperature operation

The cell was tested at higher temperature at 50C and 80C. First, the charge/discharge curves at 50C are shown in Figure B13. There was a lower IR drop of 50mV at 50C compared to 25C. SEI formation was observed at 0.8V in the first charge curve, which is the reported potential for Pyr<sub>13</sub><sup>+</sup>-FSI<sup>-</sup> reduction at graphite surface. Similar to the results at 25C, the discharge capacity increased from 150 to 240mAh/g by number of cycles. The first discharge capacity was higher at 50C than 25C. This may be because the electrolyte reduction was accelerated at higher temperature, so the lithiation occurred more in the first charge at 50C. The final capacity at 50C reached similar value at 25C. The total irreversible capacity due to the SEI formation might be similar regardless of the temperature. The capacity value remained stable from 3<sup>rd</sup> cycle in Figure B13, except the 4<sup>th</sup> and 7<sup>th</sup> cycle. The same amount of capacity drops was because of the self-discharge during the impedance measurement. When the cell operation stopped as a charged state for measurement, the discharge capacity was lower by 50mAh/g. However, the capacity at 5<sup>th</sup> cycle returned to the similar value at 3<sup>rd</sup>, indicating that it is not a capacity fading, and only a self-discharge.

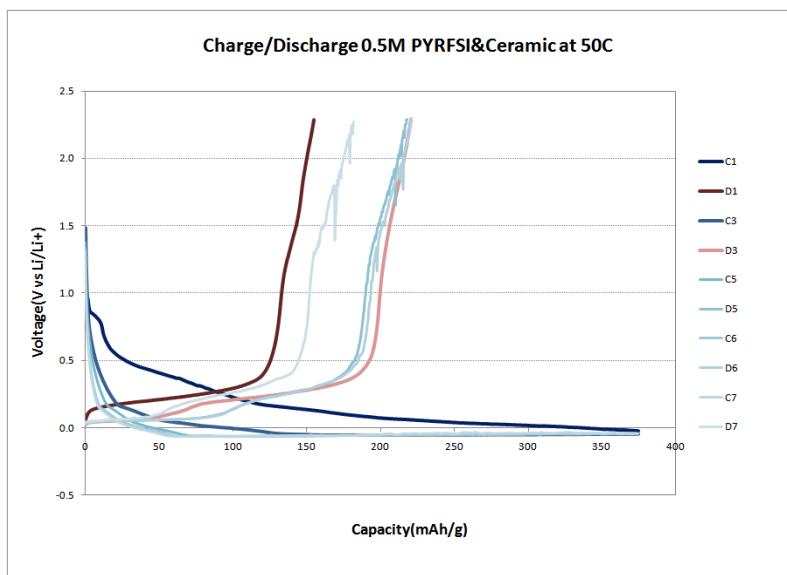


Figure B13: Charge/Discharge cycles of the cell with LiSiCON using 0.5M LiTFSI/ Pyr<sub>1R</sub><sup>+</sup>-FSI<sup>-</sup> as a contact agent (50C)

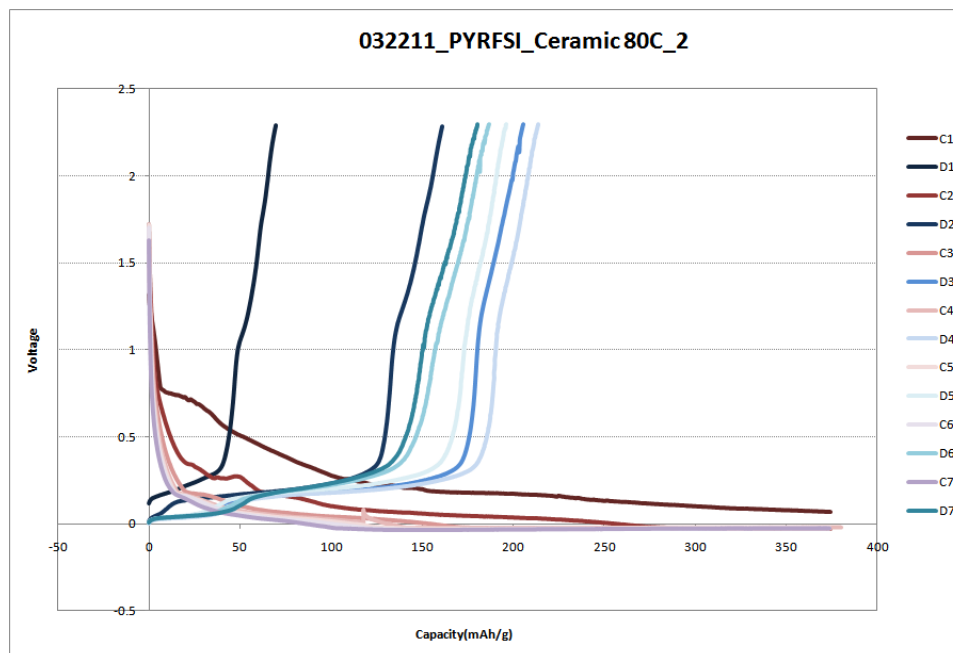


Figure B14: Charge/Discharge cycles of the cell with LiSiCON using 0.5M LiTFSI/ Pyr<sub>1R</sub><sup>+</sup>-FSI<sup>-</sup> as a contact agent (80C)

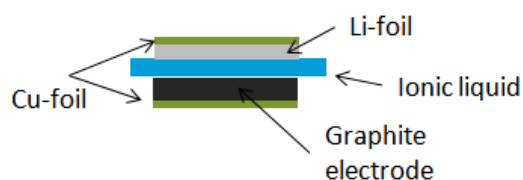
The cell was also tested at 80C shown in Figure B14. As expected, even less IR drop was observed at 80C compared to 50C and 25C. Like the results at lower temperatures, the capacity increased with cycles, and reached to the highest capacity of 220mAh/g at 4<sup>th</sup> cycle. Unlike the cell operation at 50C, there was

a capacity fade from 4<sup>th</sup> to 7<sup>th</sup> cycles. To study the reason for this capacity fade, impedance tests have been performed.

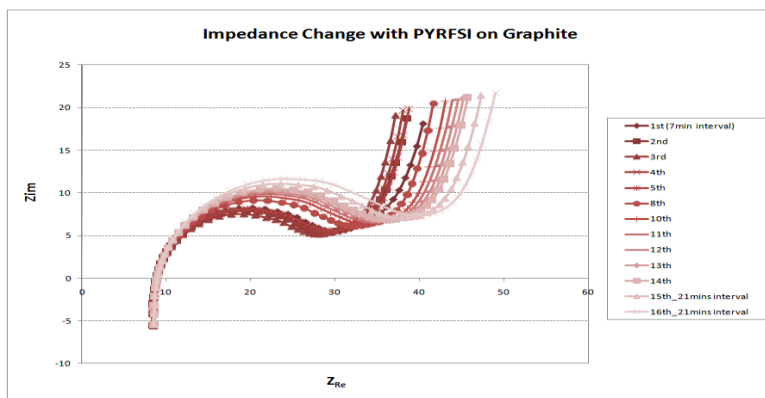
## 9. Impedance study with LiSICONs

### 9-1. Li-(ionic liquid(IL))-Graphite Cell

To study the cell resistance change during the operation, first the impedance of the cell with pure ionic liquid was studied. The cell configuration is shown in Figure B15(a) and the impedance change with time before the cell operation is in Figure B15(b). The impedance data shows a clear semicircle. The electrolyte resistance measured from the first x-intercept is around  $9\Omega$  which is corresponding to the ionic liquid resistance. Interestingly, the Rct increased slightly. The increase in Rct is due to a possible film formation in Li metal surface in contact with ionic liquid. However, the capacity calculated in Figure B15(c) did not change with time. The capacity value is in the order of  $10^{-6}$  F and should be a double layer capacity. When the cell is operated, the change in impedance is shown in Figure B15(d). After 4<sup>th</sup> cycle, the electrolyte resistance doubled due to the SEI formation on the surface of the graphite. The overall Rct also increased.



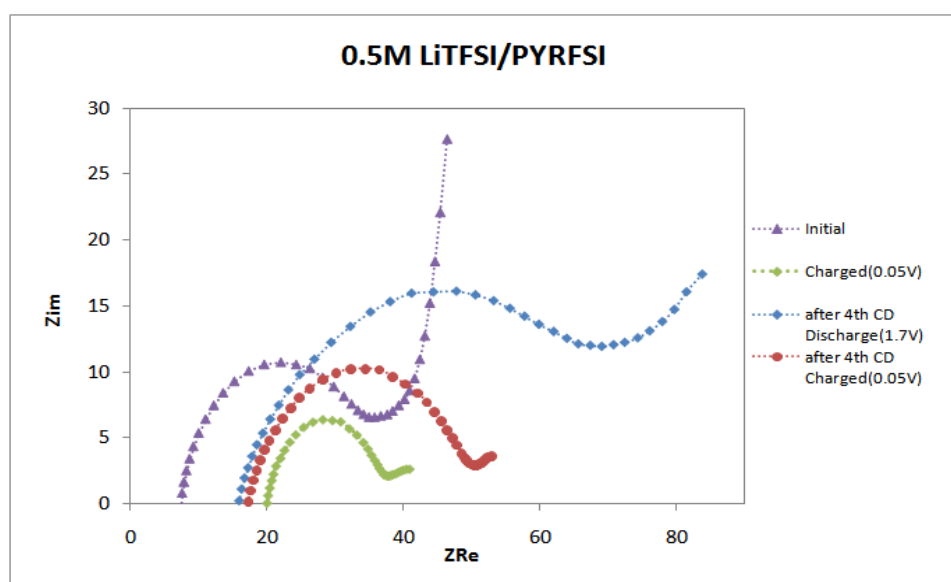
(a) Cell configuration



(b) Impedance change with time of the cell before operation

	time(min)	Re	Re+Rct/2		Rct	w(1/s)	C (F)
1	0	9.13	20.25		22.23	2778.22	2.58E-06
2	7	8.88	19.47		21.18	2778.22	2.71E-06
3	14	8.87	19.18		20.62	2778.22	2.78E-06
4	21	8.88	19.40		21.04	2778.22	2.72E-06
5	28	8.89	19.53		21.28	2778.22	2.69E-06
8	49	8.99	20.35		22.72	2778.22	2.52E-06
10	63	8.99	22.40		26.82	2218.28	2.68E-06
12	77	9.00	22.81		27.62	2218.28	2.60E-06
14	91	8.99	23.09		28.20	2218.28	2.55E-06
15	112	9.00	23.49		28.98	2218.28	2.48E-06
16	133	9.01	23.94		29.86	2218.28	2.40E-06

(C) Capacity calculation results

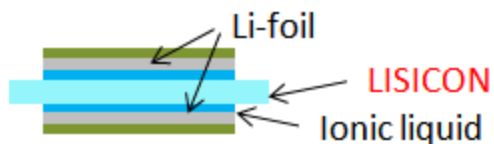


(d) Impedance change during cell operation

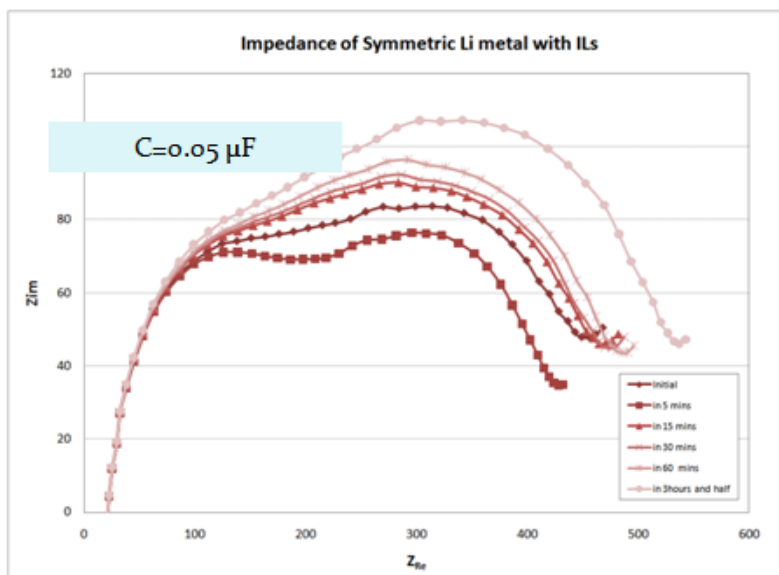
Figure B15: Li-(ionic liquid(IL))-Graphite Cell

### 9-2. Li- (LiSICON+IL)-Li Symmetric Cell

LiSICON was inserted in the cell with the 0.5M LiTFSI/ Pyr<sub>1R</sub><sup>+</sup>-FSI<sup>-</sup> as a wetting agent. First, the symmetric cell with Li metal at both sides of the LiSICON was designed to compare. The cell configuration is shown in Figure B16 (a). Interestingly, two clear arcs appeared by insertion of LiSICON in Figure B16 (b). We think the first arc is the possible RC circuit of the grain boundary with the capacity value in the magnitude of 10<sup>-8</sup> F. The second arc could be the combination of the two Li-metal electrodes, also increasing with time as seen in the Figure B16(b).



(a) Cell configuration



(b) Impedance change with time of the cell before operation and the calculated capacities

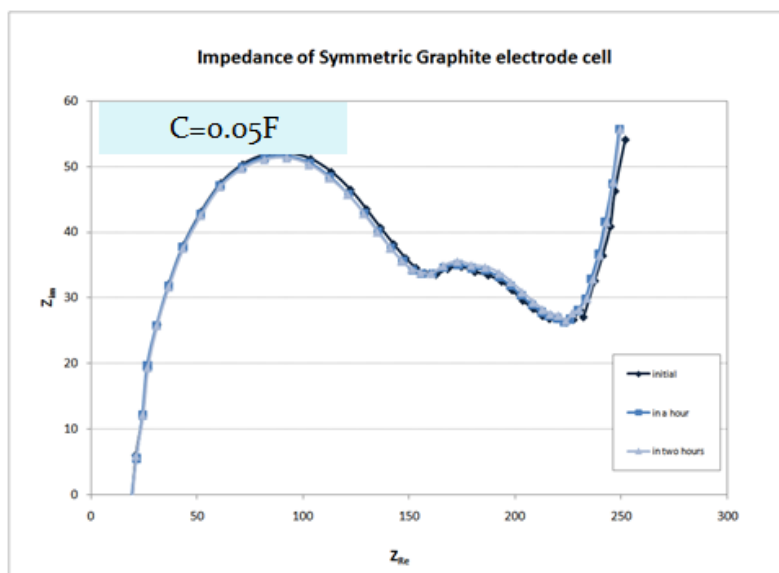
Figure B16. Li- (LiSICON+IL)-Li Symmetric Cell

### 9-3. Graphite- (LiSICON+IL)-Graphite Symmetric Cell

Next, a symmetric cell with the graphite electrodes at both sides of LiSICON, shown in Figure B17(a), was tested in a same manner. The cell impedance was observed. Figure B17(b) showed the two clear arcs like Figure B16(b). The capacity of the first arc was as same as the previous cell design, confirming that this is for the grain boundary of the LiSICON. However, the second arc did not change with time confirming that the increasing in  $R_{ct}$  is due to the Li.



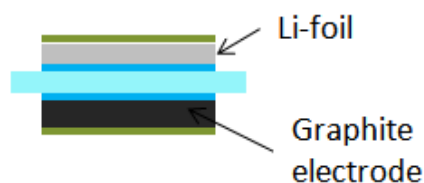
(a) Cell configuration



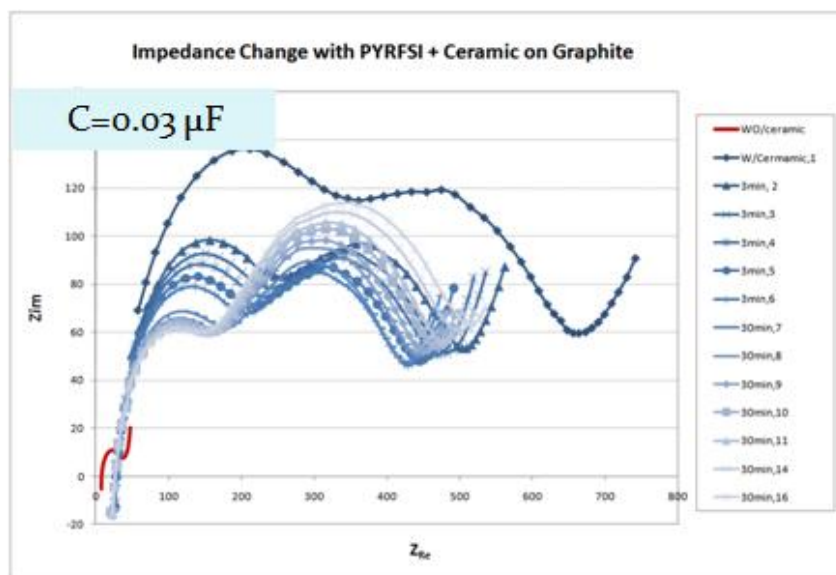
(b) Impedance change with time of the cell before operation and the calculated capacities  
Figure B17. Graphite-(LiSICON+IL)-Graphite Symmetric Cell

#### 9-4. Li- (LiSICON+IL)-Graphite Half Cell

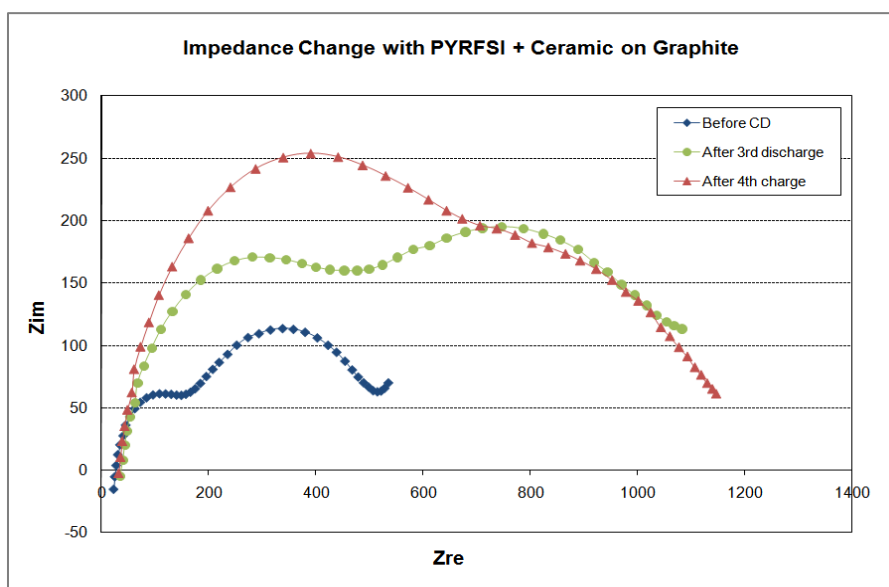
Finally, a half cell was constructed as shown in Fig B18(a) and evaluated in a same manner. The two clear semicircles were observed as in previous results. The second arc is for the combination of Li and graphite electrodes. In the presence of Li, the Rct of the second arc also increased as seen in the previous results. By comparing the capacity values of the second arc in FigureB16(b), Figure B17(b) and FigureB18(b), it can be concluded that the capacity of Li is slightly higher than graphite. In addition, the values of the first x-intercept matched, which is for the LiSICON resistance.



(a) Cell configuration



(b) Impedance change with time of the cell before operation and the calculated capacities



(c) Impedance change during cell operation

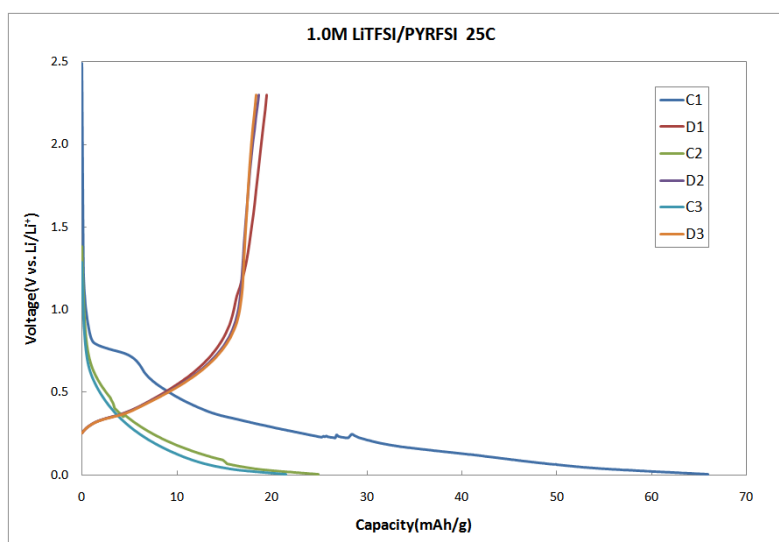
		Rct	w(1/s)	C (F)		Rct	w(1/s)	C (F)
1	initially	142.52	43287.61	2.58E-08		390.00	389.8604	1.05E-06
2	After 3 CD	439.86	19744.88	1.83E-08		740.00	231.013	9.31E-07
3	After 4C	684.92	15199.11	1.53E-08		490	300.1047	1.08E-06

(d) Capacity calculation of the arcs

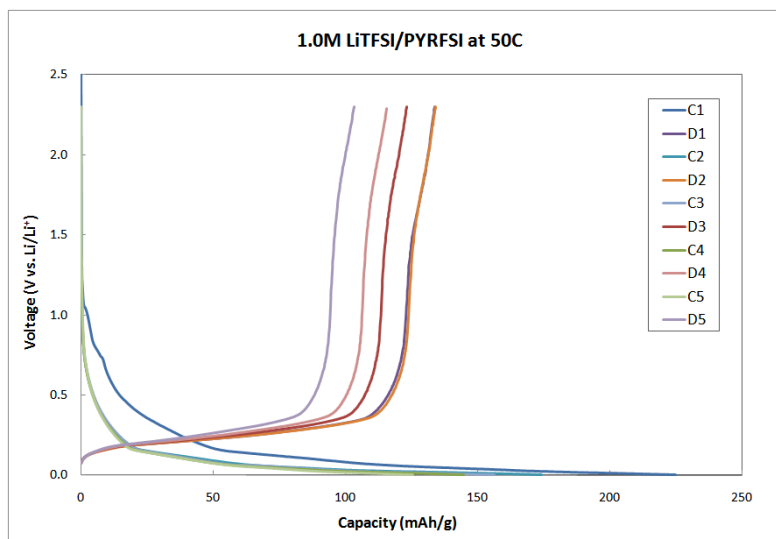
Figure B18: Graphite- (LiICON+IL)-Li Half Cell

The impedance results during the cell operation were also studied in Figure B18(d). After 3rd cycles, the resistance of the LiSICON did not change, indicating that the LiSICON was stable and the change by the SEI formation is negligible. However, the overall Rct increased after 3 cycles. The Rct of the grain boundary was also increasing, which means that the LiSICON structure might not be stable. This is maybe because of the fixed Li ion in the LiSICON was detached and changed the structure. When the Li concentration of electrolyte is lower than 1M, the fixed Li can be detached.

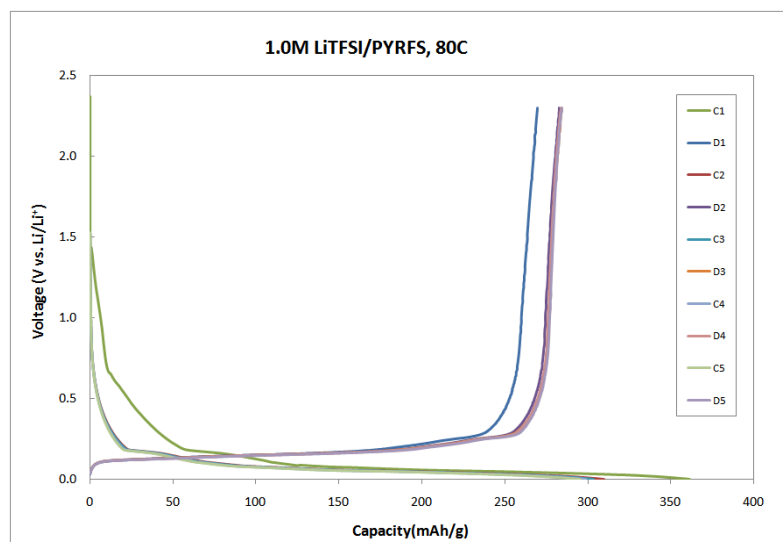
### 10. The effect of Li salt concentration



(a) 25C



(b) 50C



(C) 80C

**Figure B19: Charge/Discharge cycles using 1.0M LiTFSI/PYRFSI as a wetting agent**

Previously, 0.5M LiTFSI/PYRFSI was used as a wetting agent. However, it has been reported that the Li salt concentration can affect on the cell performance, because the concentration of the Li salt can change the conductivity of the mixture as well as viscosity and the electrochemical window. In order to see the effect of Li salt concentration, 1.0M LiTFSI/PYRFSI was used as a wetting agent. Figure B19 showed the charge/discharge cycles at C/20 at 25C, 50C and 80C. For this experiment, the potential window was set between 0V and 2.3V so there should be no concern about Li metal deposition by limiting the bottom potential as 0.01V. Compared to the results using 0.5M LiTFSI/PYRFSI shown in Figure B12, B13 and B14, 1.0M LiTFSI/PYRFSI showed better performance overall. The IR drop was lower, so finally lithiation occurred above 0V. In case of 80C, the first charge capacity is 361mAh/g and the discharge capacity is around 285mAh/g. While the capacity at 50C was decreasing by cycles, the capacity at 80C was stable. At higher temperature, the lithium ion conductivity is higher resulted in higher capacity. Without passing the 0V, the capacity at 80C showed comparable capacity to the organic solvent at room temperature.

The discharge capacities of three different Li salt concentrations were compared in Figure B20. For the experiments, 0.50M, 0.75M and 1.00M of LiTFSI was mixed with PYRFSI and five charge/discharge cycles were recorded at C/20. Among the three concentration, 0.75M showed the highest performance which is around 310mAh/g. The charge/discharge efficiency of three different concentrations is shown in Figure B21, and the highest efficiency was 99.7% with 0.75M.

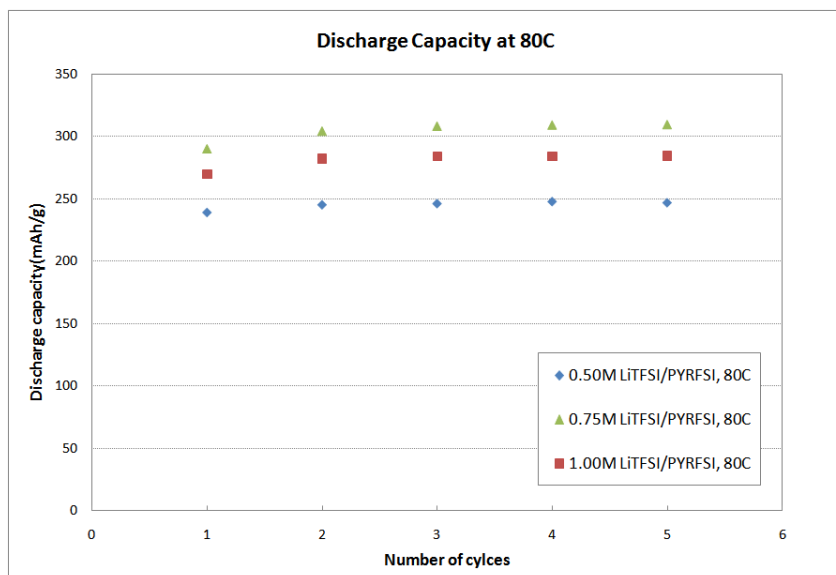


**Figure B20: The discharge capacity of three different Li salt concentrations at 80C**

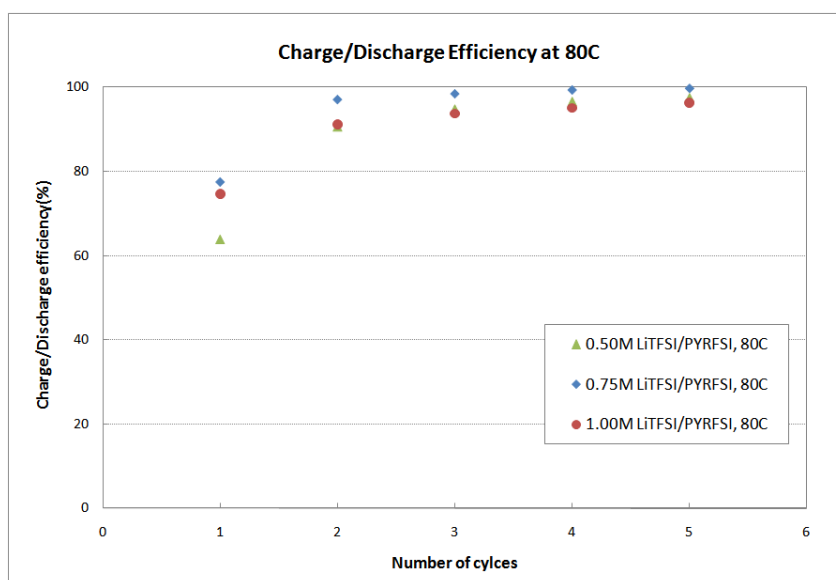


**Figure B21: The charge/discharge efficiency at 80C comparing three different concentrations**

The 0.75M electrolyte showed better performance than 0.5M. Higher the concentration, lower the ionic conductivity and higher the viscosity. It was a surprising because even though the ionic conductivity of 0.75M was lower than 0.5M, it showed better performance. In order to know the reason, first charge curves of three concentrations were compared in Figure B22. When the Li salt concentration increases, the reduction of electrolyte starts at more positive potential. The electrochemical window shift of ionic liquids by the salt concentration was reported in the literature(6). For LiTFSI/PYRFIS, the reduction potential of the mixture was shifted negatively as increasing the Li salt. The 0.5M electrolyte

reduced earlier than 0.75M and 1.0M, so more graphite was reacted to form a SEI layer and became irreversible.

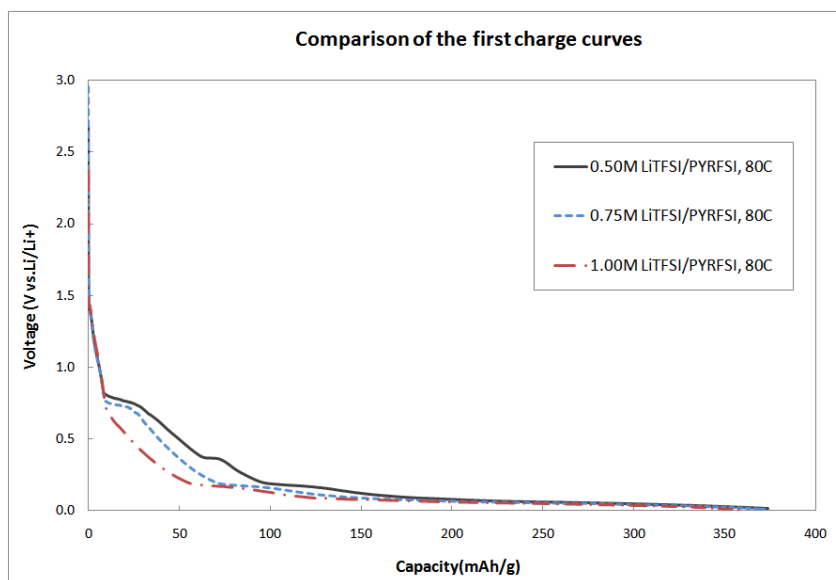
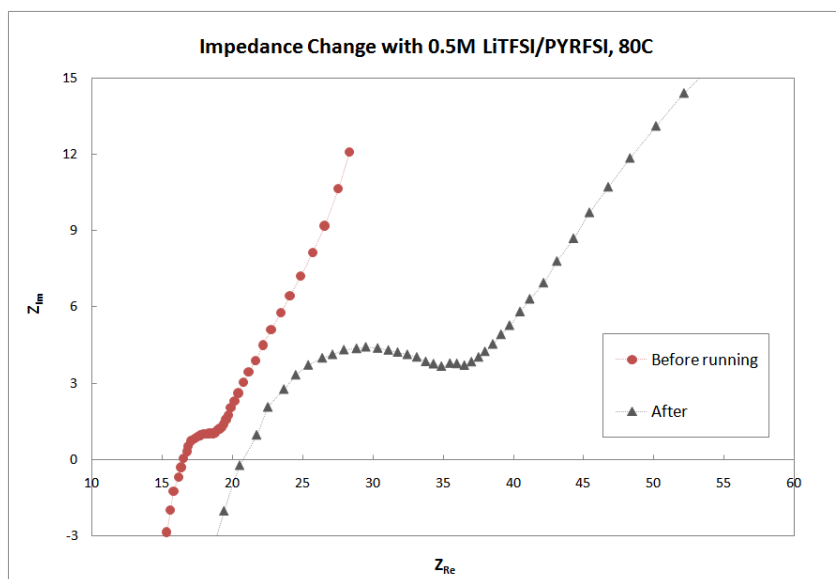
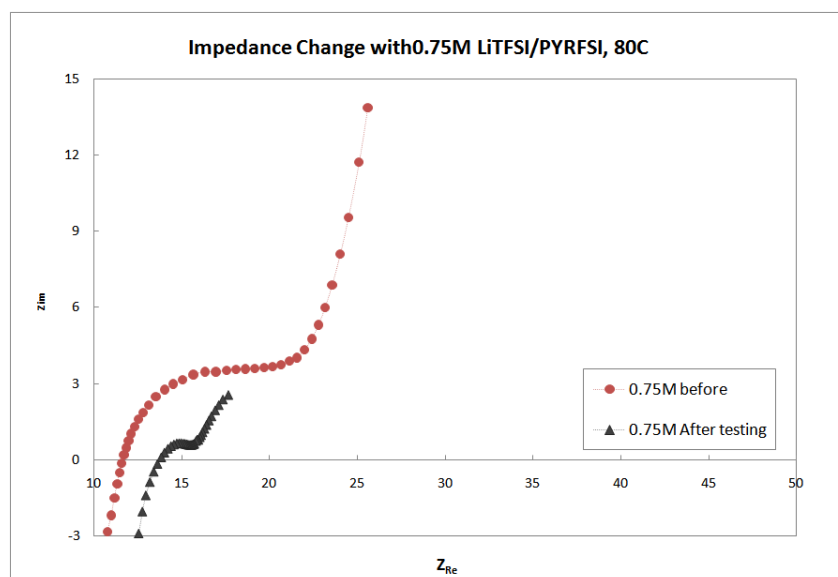


**Figure B22: The first charge curves for 0.5M, 0.75M and 1.0M LiTFSI/PYRFSI at 80C**

Figure B23 showed the impedance change of 0.5M and 0.75M before and after running the charge/discharge cycles. In both cases,  $R_b$  was increased after running the cells. It was because the electrolyte reduced and formed nonconductive SEI. The increase of  $R_b$  was higher with 0.5M than 0.75M indicating that 0.5M formed a thicker SEI. The  $R_{ct}$  of 0.5M cell was also increased after running the cycles, while the  $R_{ct}$  of 0.75M was decreased. 0.75M electrolyte formed a more stable SEI than 0.5M.



**(a) With 0.5M LiTFSI/PYRFSI**



(b) With 0.75M LiTFSI/PYRFSI

Figure B23: Impedance change before and after charge/discharge cycles

The reduction potential of the 1.0M electrolyte was lower than 0.75M, so it was expected to have better performance with 1.0M. However, the first charge curve of 1.0M in Figure B22 reached 0V faster than 0.75M providing a lower capacity. The overall discharge capacity of 1.0M was lower than 0.75M as shown in Figure B20. It might be due to the lower ionic conductivity and high viscosity of 1.0M than 0.75M. In conclusion, there are two factors affected by the Li salt concentration. One is the reduction potential and the other is the conductivity of electrolyte. It indicates that the salt concentration of the ionic liquid electrolyte needs to be optimized to have enough conductivity to fully lithiate and to form a stable SEI layer with minimum loss of the graphite.

### Summary and Future Works

LiSICON was received from CeramaTech and the conductivity of the ceramic was measured by AC impedance. As a first possible anode for LiSICON, graphite anodes were studied. Cyclic voltammetry was performed to investigate the lithiation and delithiation behavior of the graphite electrode. The graphite anode with conventional organic solvent showed higher than 96% delithiation efficiency and 320 mAh/g of charge capacity.

When the LiSICON was used as an electrolyte, the current was low and the lithiation/delithiation did not occur due to a high interfacial resistance between the LiSICON and the electrodes. Impedance analysis was used to determine which side of the electrode is largely responsible for the resistance. It

was found that the contact resistance on the graphite side was higher than that on the lithium metal side. The interfacial resistance could be reduced by using a liquid electrolyte.

To reduce the high interfacial resistance between the electrodes and LiSICON and to operate the cell, a wetting agent was necessary.  $\text{Pyr}_{1\text{R}}^+\text{-FSI}^-$  was evaluated as a wetting agent for graphite electrodes, and 0.5M LiTFSI/PYRFSI showed reversible lithiation/delithiation with efficiency of 84%. One of the big advantages using ionic liquids as a wetting agent compared to the organic solvent is that it can utilize the cells at high temperature application. At the same time the IR drop by the LiSICON can be reduced. The cell performance was evaluated at three different temperatures of 25C, 50C and 80C. As increasing the temperature, the IR drop from the LiSICON was reduced, so the lithiation occurred at higher potential. In all cases, the discharge capacity increased with cycles and reached its maximum value at the 3<sup>rd</sup> cycle.

To understand the behavior of cell operation, impedance study was performed. When LiSICON was inserted, two semicircles were clearly observed. It was found out that the first arc could be possible RC circuit of grain boundary in LiSICON showing a capacity around  $10^{-8}\text{F}$ . The second semicircle is for the combination of the electrodes, and the  $R_{\text{ct}}$  of the second one was increasing with time when the Li-meal was present. The increase in  $R_{\text{ct}}$  is due to a possible film formation in Li metal surface in contact with ionic liquid. After the 3<sup>rd</sup> charge/discharge cycle, there was negligible change in the bulk resistance. However, the  $R_{\text{ct}}$  of the grain boundary seems to increase. This is maybe because of the fixed Li ion in the LiSICON was detached and change the structure. When the Li concentration of electrolyte is lower than 1M, the fixed Li can be detached. Future works include the study on the effect of the Li concentration in the contact agent on the  $R_{\text{ct}}$  of grain boundary.

It has been reported that the Li salt concentration affects the ionic conductivity and the electrochemical window of the electrolyte. The effect of salt concentration on charge/ discharge capacity and efficiency at 25C, 50C and 80C was studied. It was found that 0.75M showed better performance than 0.5M. Because the reduction potential of the electrolyte was shifted positively by increasing the salt concentration, 0.5M electrolyte reduced earlier than 0.75M reacting with more graphite. It resulted in higher amount of irreversible capacity. Although 1.0M reduced later than 0.75M, it showed lower capacity since it reached 0V earlier than 0.75M. As increasing the salt concentration, the conductivity decreased resulting in lower capacity. At 80C the LiSICON cell with 0.75M LiTFSI/PYRFSI as a wetting agent, the discharge capacity of 310mAh/g and the efficiency of 99.7% were successfully achieved.

For future works, lithium metal anode can be the second possible anode with the LiSICON electrolyte. The short-circuit by dendrite growth can be prevented by the solid LiSICON. Also, the usage of wetting agent at the interface of Li-metal and LiSICON can prevent the unstable black layer formation. The biggest advantage of LiSICON with Li-metal anode is that it can utilize any type of cathodes, such as aqueous based  $\text{Ni}(\text{OH})_2$  cathode for Li-Ni battery and air cathode for Li-Air battery. In addition, it can be used for higher temperature molten lithium battery. In this case, the wetting agent is not necessary because the liquid Li can keep constant contact with the LiSICON.

### References

1. T. Hirai, I. Yoshimatsu and J. Yamaki, *J Electrochem Soc*, **141**, 611 (1994).
2. M. Ishikawa, T. Sugimoto, M. Kikuta, E. Ishiko and M. Kono, *J Power Sources*, **162**, 658 (2006).
3. T. Sugimoto, Y. Atsumi, M. Kikuta, E. Ishiko, M. Kono and M. Ishikawa, *J Power Sources*, **189**, 802 (2009).
4. J. H. Kennedy and Z. M. Zhang, *Solid State Ionics*, **28**, 726 (1988).
5. P. Knauth, *Solid State Ionics*, **180**, 911 (2009).
6. A. S. Best, A. I. Bhatt and A. F. Hollenkamp, *J Electrochem Soc*, **157**, A903 (2010).